

Growth, Spectral, Optical and Antibacterial Activity Studies on Glycine Hydrofluoride Single Crystal

C. Muthuselvi^{1*}, S. Manisha¹, R. S. Prabha¹

¹Department of Physics, Devanga Arts College, Aruppukottai- 626 101, Tamilnadu, India

*Corresponding Author: Dr. C. Muthuselvi,

Abstract

The glycine complexes with inorganic acid have been of particular interest because they play the widespread roles in the nonlinear optical applications. This study will help the researcher to develop physical property, chemical stability, linear and nonlinear optical properties of the materials. So, an attempt was made using the slow evaporation method on the growth of glycine hydrofluoride single crystal. The structural, vibrational, optical, morphology and the antibacterial activity studies are discussed in the present work.

Keywords: Glycine complexes, Hydrofluoric acid, XRD, IR, Raman, UV, Antimicrobial activity, SEM, EDX.

Date of Submission: 12-11-2020

Date of acceptance: 28-11-2020

I. INTRODUCTION

The indispensable amino acid of glycine is a significant component of structural proteins, enzymes and hormones [1, 2]. It is ambivalent, meaning that it can be inside or outside of the protein molecule [3]. The glycine molecule will crystallizes into three polymorphic zwitterions α , β and γ in the aqueous solution [4]. Depending on pH value glycine molecule can espouse a cationic, zwitterionic, or anionic form [5]. For the recent decades, materials explored for NLO applications are mostly inorganic [6]. The glycine complexes with inorganic salts have been already reported by many researchers due to its proficient nonlinear optical efficiency [7-11]. During our on-going study dealing with the search of new glycine complexes with the inorganic acids, we have recently studied and reported the glycinium dihydrogen phosphate [12], bis glycine hydrobromide [13] and diglycine perchlorate [14] systems whereas, the present paper deals with the glycine hydrofluoride system. Some papers committed to this system were studied and they have been reported by Khandpekar [15], Fleck et al.[16] and Vijayan et al.[17]. By considering some significant applications of the single crystal in materials science, we focus our attention on the growth of glycine hydro fluoride single crystal by the slow evaporation technique. The grown crystal is characterized by single crystal XRD, powder XRD, FT-IR, FT-Raman, UV-Visible spectroscopy, SEM with EDX and antimicrobial activity studies. The results of these studies have been discussed in this paper.

II. MATERIALS AND METHODS

The glycine and hydrofluoric acid were purchased from Sigma Aldrich Company, India. Initially an aqueous solution containing glycine [$\text{NH}_2\text{CH}_2\text{COOH}$] and hydrofluoric acid [HF] were prepared in the molar ratio of 1:1. The solution was stirred well for 1 hour and poured into the plastic vessels (ie. polyethylene). Since the solutions containing hydrofluoric acid react with glass. The chemical reaction takes place as

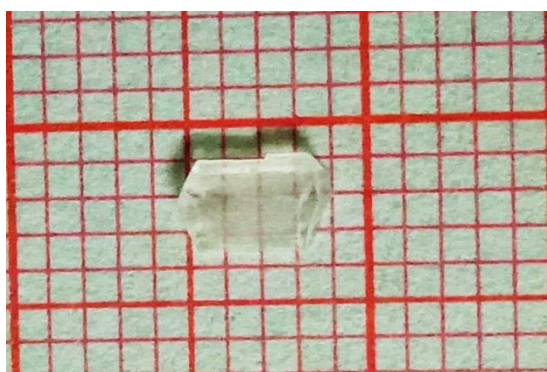
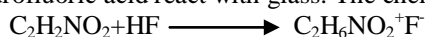


Fig. 1: Grown crystal of glycine hydrofluoride

The crystals were obtained after 25 days by slow evaporation technique at room temperature. The photographic view of grown crystal is depicted in Fig. 1.

The good quality crystal was selected to carry out the single crystal X-ray diffraction using Bruker SMART APEX CCD diffractometer with MoK α radiation ($\lambda = 0.71073 \text{ \AA}$). The powder diffraction pattern was recorded using XPERT-PRO X-ray diffractometer with CuK α ($\lambda = 1.54060 \text{ \AA}$) radiation. Using SHIMADZU FT-IR spectrometer, vibrational spectrum was recorded in the range 4000–400 cm^{-1} . Also, the FT-Raman spectrum was recorded using the BRUKER: RFS 27 Raman spectrometer in the wavenumber range 4000–400 cm^{-1} . The optical absorption spectrum of glycine hydrofluoride crystal has been recorded with SHIMADZU-UV1800 double beam spectrometer in the wavelength range 200–1100 nm in steps of 1nm. The surface morphology and elemental analysis has been carried out by CARLZEISS EVO18 scanning electron microscope. Also, using the disc diffusion method, the antibacterial activity study was analyzed against four different kinds of micro-organisms (Micrococcus, S. Typhi, B. Subtilis and Pseudomonas).

III. RESULT AND DISCUSSION

3.1. Single crystal XRD analysis

The single-crystal X-ray diffraction analysis was carried out to identify the lattice parameters of the grown crystal. The estimated lattice parameter values were checked in the Cambridge Structural Database (CSD) for confirmation. The report showed that the grown crystal is exactly matched with already reported values by Selvaraju et al. [18]. The experimental values of title compound are tabulated in Table 1 and compared with the available reported literature values [18].

Table 1: Lattice parameters value of glycine hydrofluoride crystal

Lattice parameters	Present study	Already reported [18]
Compound name	Glycine hydrofluoride	Glycine hydrofluoride
Empirical formula	C ₂ H ₆ NO ₂ ⁺ · F ⁻	C ₂ H ₆ NO ₂ ⁺ · F ⁻
Molecular weight	250.60	250.60
Unit cell dimensions	a = 5.4887 (3) (Å) b = 7.6615 (2) (Å) c = 8.8545 (3) (Å) $\alpha = \beta = \gamma = 90^\circ$	a = 5.4896 (2) (Å) b = 7.6617 (2) (Å) c = 8.85562 (2) (Å) $\alpha = \beta = \gamma = 90^\circ$
Volume	359.7804 (8) (Å) ³	359.8706 (7) (Å) ³
Crystal system	Orthorhombic	Orthorhombic

The orthorhombic structure of glycine hydrofluoride is observed from the single crystal XRD analysis. The molecular structure of glycine hydrofluoride is shown in Fig. 2.

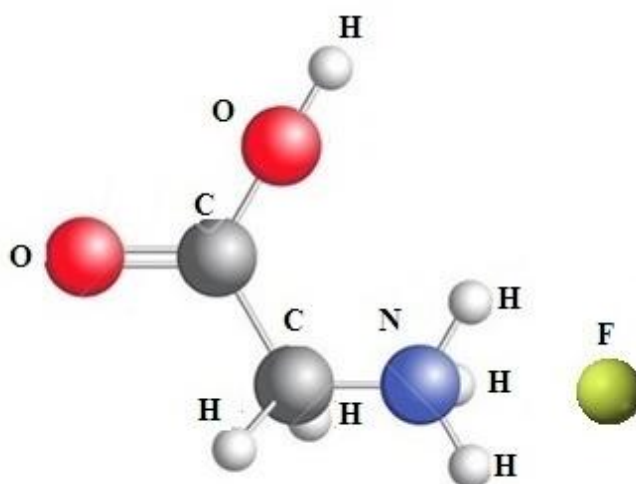


Fig. 2: Molecular structure of glycine hydrofluoride single crystal

3.2. Powder XRD analysis

The powder diffraction data was collected for glycine hydrofluoride single crystal and the experimentally recorded PXRD pattern is shown in Fig. 3. The appearance of sharp and strong peaks recognized the good crystalline nature of the grown crystal. The characteristic peak of this compound has appeared at 30.20°. The INDX software is used to index the PXRD pattern. The average crystalline size is determined from the Debye-Scherrer equation, which can be written as,

$$D = \frac{K\lambda}{\beta \cos\theta}$$

Where,

D - Average crystallite size

K- Dimensionless shape factor (0.94)

λ - Wavelength of X-ray radiation (CuK α = 1.54060 Å)

θ -Diffraction angle

β -Full width at half maximum intensity

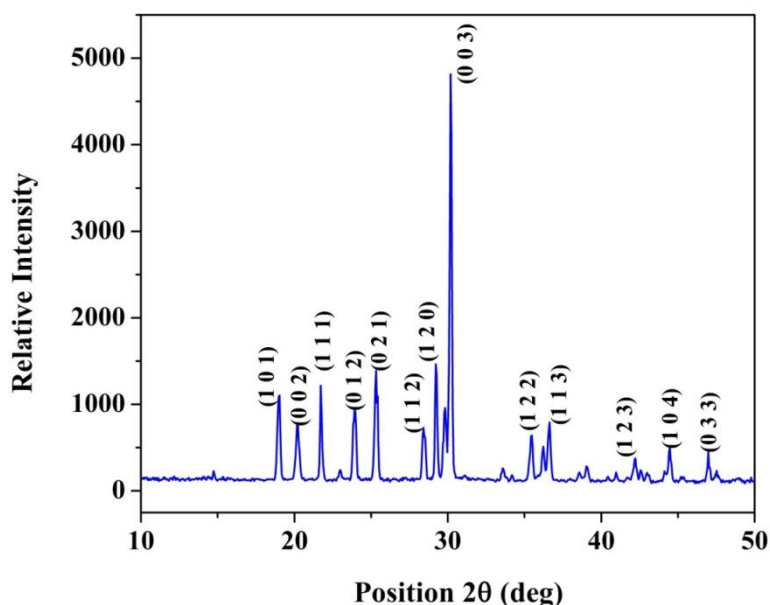


Fig. 3: Diffraction patterns for glycine hydrofluoride crystal

The dislocation density can be calculated from,

$$\delta = \frac{1}{D^2} \text{ m}^2$$

Where,

δ - Dislocation density

D - Crystallite size

The average crystalline size is found to be as 56 nm for title crystal. Also, the dislocation density is determined as $8.15 \times 10^{14} \text{ m}^{-2}$.

3.3. FT-IR and FT-Raman Vibrational analysis

The experimentally recorded FT-IR and FT-Raman spectra of glycine hydrofluoride crystal are shown in Fig. 4 and Fig. 5 respectively. It has — $[\text{NH}_3]^+$, CH_2 , C—C, C—N and COOH functional groups. The detailed wavenumber assignment is presented in Table 2.

3.3.1. Carboxylic group vibrations

The antisymmetric and symmetric stretching modes of C=O group has identified in the region $1720\text{--}1680 \text{ cm}^{-1}$ and $1680\text{--}1640 \text{ cm}^{-1}$ respectively [19]. There is no counterpart in both spectra for $\nu_{\text{as}}(\text{C}=\text{O})$ mode. The sharp and intense bands appear at 1658 cm^{-1} in IR and at 1667 cm^{-1} in Raman spectra is assigned to the $\nu_{\text{s}}(\text{C}=\text{O})$ mode. The O—H stretch from CO—OH group is recognized at $3065\text{--}2826 \text{ cm}^{-1}$ [19]. This mode is accredited at 3008 cm^{-1} in Raman spectrum only. The in-plane and out-of-plane bending wavenumber of O—H group appears in the region $1440\text{--}1395 \text{ cm}^{-1}$ and $960\text{--}875 \text{ cm}^{-1}$ respectively [19, 20]. In the present work, $\beta(\text{O}\text{--H})$ mode is attributed at $1447, 1410 \text{ cm}^{-1}$ in IR and at $1447, 1407 \text{ cm}^{-1}$ in Raman spectra respectively. Also $\gamma(\text{O}\text{--H})$ mode is ascribed at $895, 891 \text{ cm}^{-1}$ in both spectra for the title compound.

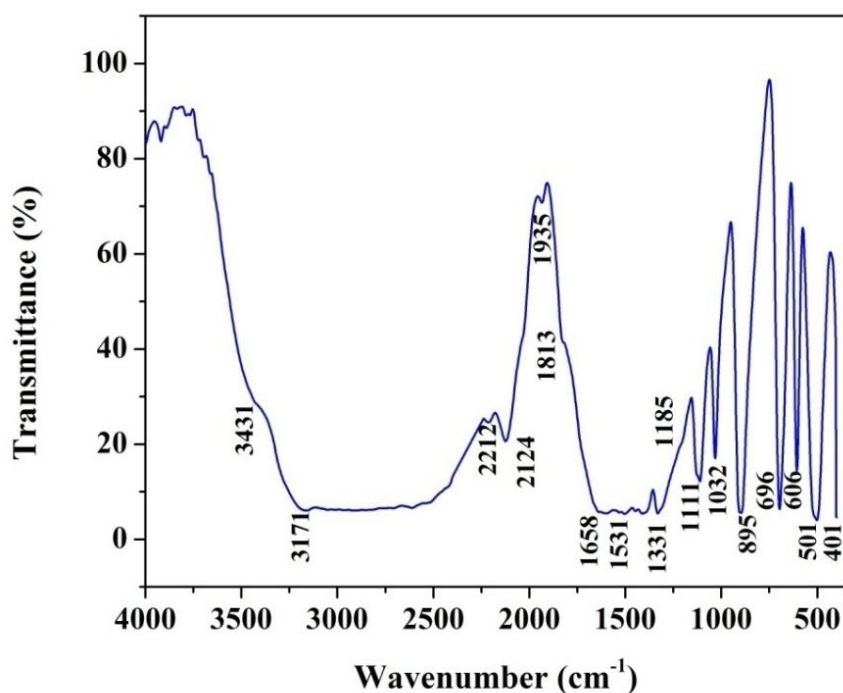


Fig. 4: FT-IR spectrum of glycine hydrofluoride crystal

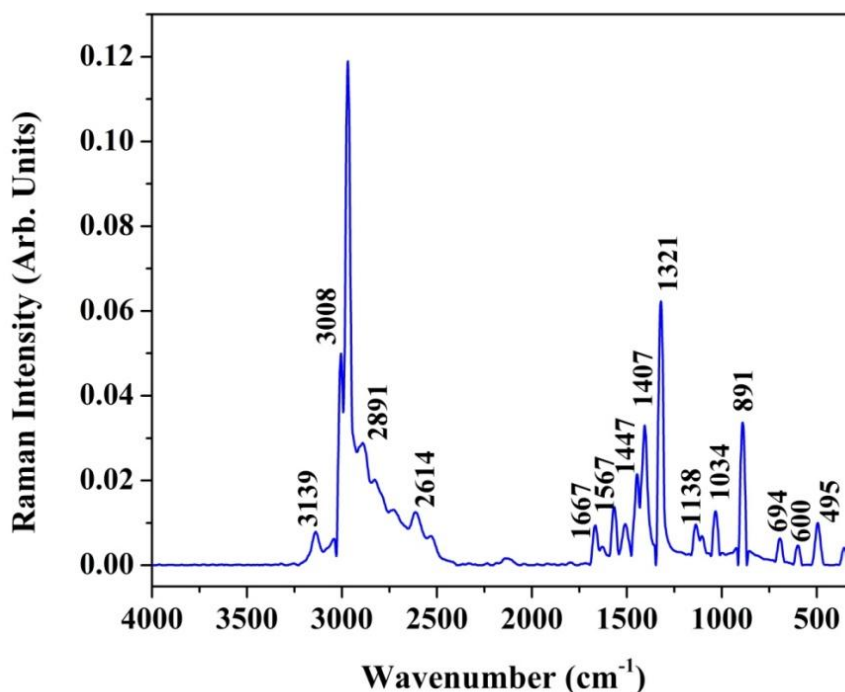


Fig. 5: FT-Raman spectrum of glycine hydrofluoride crystal

3.3.2. CH₂ group vibrations

The CH₂ antisymmetric and symmetric stretching vibrations can exist in the region of 3000–2900 cm⁻¹ and 2900–2800 cm⁻¹ respectively [21-23]. The $\nu_{as}(\text{CH}_2)$ and $\nu_s(\text{CH}_2)$ modes are accredited at 2969 cm⁻¹ and 2891 cm⁻¹ in the Raman spectrum only. The scissoring, wagging and twisting modes of CH₂ fall in the array 1482–1437 cm⁻¹, 1390–1180 cm⁻¹ and 730–720 cm⁻¹ respectively [24]. The bands appear at 1447 cm⁻¹ in both

spectra is assigned to CH₂ scissoring mode. Also, the wagging mode is attributed at 1331 cm⁻¹ (IR), 1321 cm⁻¹(Raman). The twisting and rocking modes are not conceding for the title compound.

Table 2: Wavenumber assignments for glycine hydrofluoride crystal in FT-IR and FT-Raman spectra

FT – IR ($\bar{\nu}$ / cm ⁻¹)	FT– Raman ($\bar{\nu}$ / cm ⁻¹)	Assignment
3174 (s, br)	3139 (w)	$\nu_{as}[\text{NH}_3]^+$
-	3008 (s)	ν (O–H)
-	2969 (s)	$\nu_s[\text{NH}_3]^+$; ν_{as} (CH ₂)
-	2891 (m)	$\nu_s[\text{NH}_3]^+$
1658 (m)	1667 (m)	ν_s (C=O)
1534 (s)	1567(m)	$\delta_{as}[\text{NH}_3]^+$
1541 (s)	-	$\delta_s[\text{NH}_3]^+$
1503 (s)	1509(m)	$\delta_s[\text{NH}_3]^+$
1447 (s)	1447 (s)	ρ (CH ₂); β (O–H)
1409(s)	1407 (s)	β (O–H)
1331(s)	1321 (s)	ω (CH ₂)
1131(sh)	1137 (w)	ν (C–N)
1032 (m)	1036 (m)	ν (C–C)
895 (m)	891 (s)	γ (O–H); ν (C–C)

w-weak; s- strong; m- medium; sh- shoulder; ν - stretching; ν_s - symmetric stretching;
 ν_{as} -anti symmetric stretching; δ_s - symmetric bending; δ_{as} - antisymmetric bending;
 γ - out-of-plane bending; β - in-plane bending; ω -wagging.

3.3.3-[NH₃]⁺ group vibrations

The $-\text{[NH}_3\text{]}^+$ group antisymmetric and symmetric stretching modes are establish in the range of 3200 and 2800 cm⁻¹ respectively [25] . The strong broad band appears at 3174 cm⁻¹ in IR and a weak band at 3139 cm⁻¹ in Raman spectra is assigned to the $\nu_{as} -\text{[NH}_3\text{]}^+$ mode. The $\nu_s-\text{[NH}_3\text{]}^+$ mode is ascribed at 2969, 2891 cm⁻¹ in Raman spectrum, there is no corresponding wavenumber in IR spectrum for this mode . The antisymmetric and symmetric deformation modes of $-\text{[NH}_3\text{]}^+$ group are expected in the region of 1625–1550 cm⁻¹ and 1550–1505 cm⁻¹ respectively [25, 26]. The $\delta_{as}-\text{[NH}_3\text{]}^+$ wavenumber is assigned at 1667 cm⁻¹ in Raman spectra. Also, the $\delta_s-\text{[NH}_3\text{]}^+$ mode is attributed at 1531, 1503 cm⁻¹ in IR and at 1567, 1509 cm⁻¹ in Raman spectra. The broad band centered at 3000 cm⁻¹ in IR spectrum is attributed to the presence of extensive three dimensional hydrogen bonding network that exists in the crystal.

3.3.4. C–C and C–N group vibrations

The stretching and bending modes of C–C normally fall in the range 1117–870 cm⁻¹ [27, 28]. For aliphatic amines, C–N absorption bands emerge in the region 1250–1020 cm⁻¹²⁸. In the present study, the bands identified at 1032, 895 cm⁻¹ in IR spectrum and at 1034, 891 cm⁻¹ in Raman spectrum is assigned to the ν (C–C) mode. Also, the ν (C–N) mode is endorsed at 1131 cm⁻¹ in IR spectrum and at 1138 in cm⁻¹ Raman spectrum.

3.4. Optical study

The absorbance spectrum of glycine hydrofluoride crystal was recorded using SHIMADZU–UV1800 double beam spectrometer in the wavelength range 200–1100 nm (Fig. 6).

The lower cut-off wavelength is found at 237 nm and it has 100% transmittance in the entire visible region which makes usefulness of this material in optical application. The Tauc's plot method is widely used for the determination of optical band gap using relation $(\alpha h\nu)^2 = A(h\nu - E_g)$. The plot is drawn for $(\alpha h\nu)^2$ against the photon energy (hν) and extrapolate the linear portion of $(\alpha h\nu)^2$ to the photon energy axis directly gives the optical band gap (E_g) of title crystal. From the Fig. 7, the optical band gap value is found as 5.7 eV which reveals that the glycine hydrofluoride crystal is a typical of dielectric material.

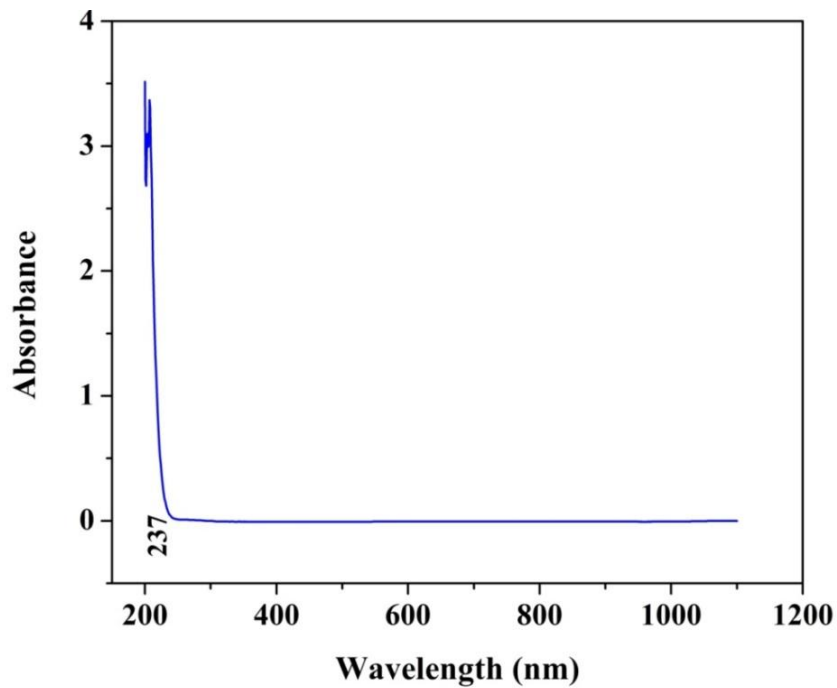


Fig. 6: Absorbance spectrum for glycine hydrofluoride crystal

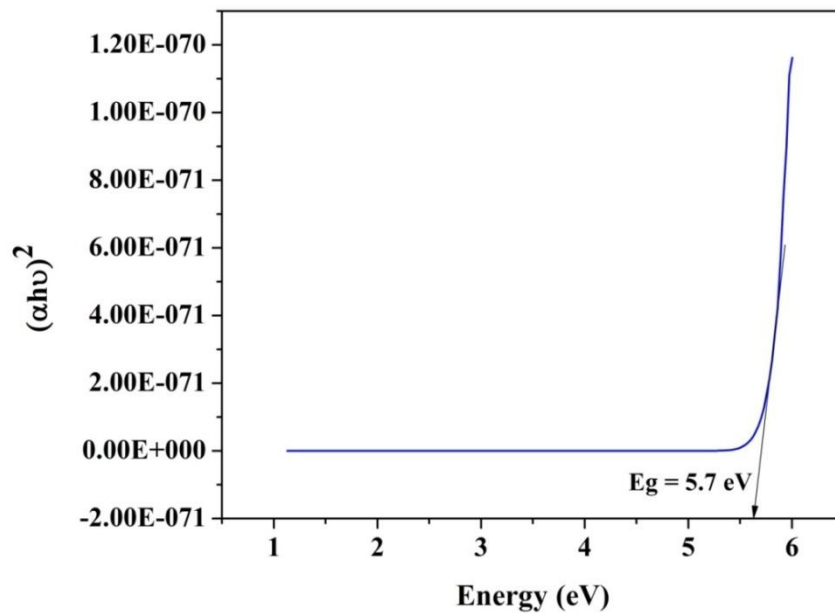


Fig. 7: Optical band gap for glycine hydrofluoride crystal

3.5. SEM with EDX analysis

The morphology and compositional analyzes were performed by SEM with EDX. The SEM images of glycine hydrofluoride crystal with two different magnifications are illustrated in Fig.8.

The SEM images reveal that the grown crystal has the well-defined shape. The EDX spectrum for crystal glycine hydrofluoride is exposed in Fig.9. Table 3 shows the elemental composition present in glycine hydrofluoride crystal. The presence of C, N, O and F elements in glycine hydrofluoride crystal is confirmed from the EDX study.

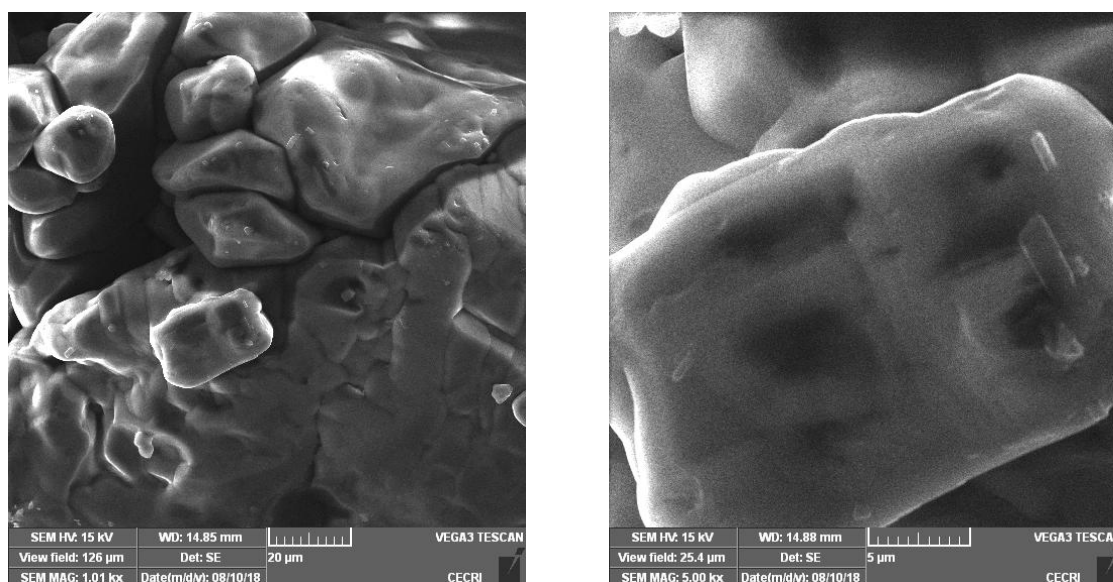


Fig. 8: SEM photograph for glycine hydrofluoride crystal

Table 3: Elemental composition for glycine hydrofluoride crystal

Elements	Glycine hydrofluoride	
	Atomic %	Weight %
C	32.9	27.7
N	21.5	21.1
O	45.3	50.8
F	0.3	0.4

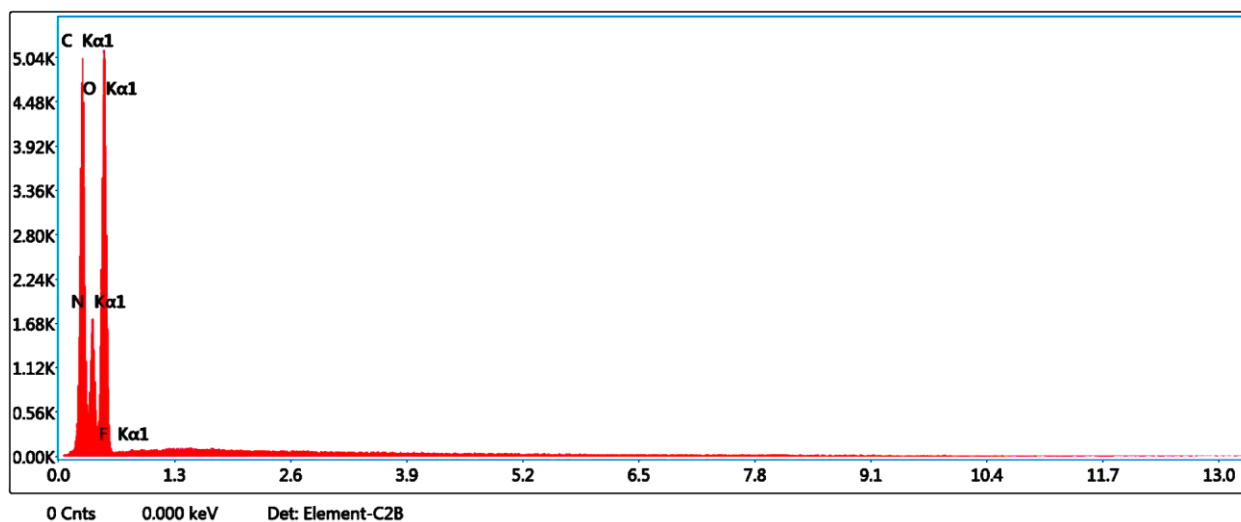


Fig. 9: EDX spectrum for glycine hydrofluoride crystal

3.6. Antimicrobial activity study

The bacterial screening effects of glycine hydrofluoride crystal were tested against *Micrococcus*, *Salmonella Typhi* and *Bacillus Subtilis*, *Pseudomonas* micro-organisms using the disc diffusion method. Fig.10 shows the bacterial screening for title crystal with 50µg/ml and 100 µg /l concentrations. The antimicrobial potential was expressed as the diameter of the growth inhibition zone in mm. Table 4 shows the results of antimicrobial activity studies. The glycine hydrofluoride crystal has no antimicrobial activity against four different test bacteria.



Fig. 10: Photographic view showing inhibition region of four different micro-organisms at 50µg/ml and 100 µg/l concentrations against glycine hydrofluoride crystal

Table 4: Effective inhibited zone values for glycine hydrofluoride crystal

S.NO.	Micro-organisms	Zone of inhibition for glycine hydrofluoride crystal	
		50 µl (mm)	100 µl (mm)
1.	Micrococcus	NIL	NIL
2.	Salmonella Typhi	NIL	NIL
3.	Bacillus Subtilis	NIL	NIL
4.	Pseudomonas	NIL	NIL

*NIL- No antimicrobial activity; mm- Zone of inhibition

IV. CONCLUSION

The optically transparent single crystals of glycine hydrofluoride were grown by slow evaporation technique at room temperature. The lattice parameter values were obtained from the single crystal XRD. In addition to single crystal XRD, powder X-ray diffraction analysis was carried out and the peaks were indexed using INDX software. The presence of $— [NH_3]^+$, CH_2 , $C—C$, $C—N$ and $COOH$ functional groups were confirmed from the FT-IR and FT-Raman spectroscopy analysis. Optical transmittance and the lower cut-off wavelength were identified using the UV-Vis-NIR spectrum. From the optical study, the optical band gap was determined as 5.7 eV. The SEM with the EDX study confirms the true composition of elements present in the glycine hydrofluoride crystal. The antimicrobial activity study exposed that the glycine hydrofluoride complex crystal has no bacterial screening effect against certain four different micro-organisms

ACKNOWLEDGEMENT

The authors sincerely acknowledge their thanks to the Management and Principal of Devanga Arts College, Aruppukottai, India for their permission and encouragement during their research work.

REFERENCES

- [1]. Yongqing Hou, Yulong Yin and Guoyao Wu, 2015. Dietary essentiality of nutritionally non-essential amino acids for animals and humans. *Exp. Biol. Med.*, 240(8):997-1007.
- [2]. Yongqing Hou and Guoyao Wu, 2018. Nutritionally Essential Amino Acids. *Adv. Nutr.*, 9(6): 849–851.
- [3]. <http://www.biology.arizona.edu>.
- [4]. Gianluca Di Profio, Mika T. Reijonen, Rocco Caliendo, Antonietta Guagliardi, Efrem Curcio and Enrico Drioli, 2013. Insights into the polymorphism of glycine: membrane crystallization in an electric field. *Phys. Chem. Chem. Phys.*, 15:9271-9280.
- [5]. Koteeswari Pandurangan and Sagadevan Suresh, 2014. Synthesis, Growth, and Characterization of Bisglycine Hydrobromide Single Crystal. *Journal of Materials*, 2014:1-7.
- [6]. Dhatchaiyini, M.K., G. Rajasekar and A. Bhaskaran, 2019. Synthesis, growth, optical, photoconductivity and specific heat properties of potassium borodicitrate (KBDC) single crystal. *J. Mater. Sci.*, 54: 9362–9371.
- [7]. Suresh Kumar, M., K. Rajesh, G.V. Vijayaraghavan and S. Krishnan, 2018. Structural and mechanical properties of diglycine perchlorate single crystals, *Materials Science-Poland.*, 36(4): 733-738.
- [8]. Ghazaryan, V.V., M. Fleck and A.M. Petrosyan, 2010. Crystal structures and vibrational spectra of novel compounds with dimericglycine glycinium cations *Journal of Molecular Structure*, 977: 117–129.
- [9]. Boopathi, K., P. Rajesh, P. Ramasamy and Prapun Manyum, 2013. Comparative studies of glycine added potassium dihydrogen phosphate single crystals grown by conventional and Sankaranaryanan–Ramasamy methods. *Optical Materials*, 35:954–961.
- [10]. Sampath Krishnan, S., N. Balamurugan, R. Kumutha, Y. Vidhyalakshmi, and R. Muthu, 2012. Growth and characterization of new nonlinear optical bis-glycine hydrobromide single crystal. *J. Min. Mater. Charact. Eng.*, 11: 597–607.
- [11]. Ambujam, K., and P. Sagayaraj, 2006. Growth and characterization of a novel NLO crystal Bis glycine hydrogen chloride, *J. Cryst. Growth.*, 286(2): 440–444.
- [12]. Muthuselvi, C., B.Sumathi and B. Ravikumar, 2018. Spectral and Antimicrobial Activity Studies on Bis Glycine Hydro Bromide Semi-Organic Crystal. *The Pharmaceutical and Chemical Journal*, 5(5):35-45.
- [13]. Muthuselvi, C., P. Uma Maheswari and B. Ravikumar, 2018. Growth, Vibrational and Antimicrobial Activity Studies on Glycinium Dihydrogen Phosphate Complex Crystal. *The Pharmaceutical and Chemical Journal*, 5(5):23-34.
- [14]. Muthuselvi, C., N. Rathika and K. Selvalakshmi, 2019. Vibrational, Optical and Antimicrobial Activity Studies on Diglycine Perchlorate Single Crystal, *Journal of Applied Sciences*, 19: 848-856.
- [15]. Khandpekar, M.M., Thermal Evaporation of Diglycine Hydrogen Fluoride Crystals, 2003. *Indian Journal of Pure and Applied Physics*, 41:704-706.
- [16]. Fleck, M., V.V. Ghazaryan and A.M. Petrosyan, 2010. Glycine hydrogen fluoride: Remarkable hydrogen bonding in the dimeric glycine glycinium cation, *Journal of Molecular Structure*, 984: 83–88.
- [17]. Vijayan, N., G. Bhagavannarayana. S. N. Sharma and Subhasis Das, 2009. Synthesis, growth and structural perfection of nonlinear optical material of glycine hydrofluoride, *J. Mater.Sci.*, 44:3457–3461
- [18]. Selvaraju, K., R. Valluvan and S. Kumararaman, 2006. New nonlinear optical material: Glycine Hydrofluoride, *Materials Letters*, 60: 2848–2850.
- [19]. Silverstein, R.M., F. X. Webster, D. J. Kiemle and, D. L. Bryce, 2014. *Spectrometric Identification of Organic Compounds*, John Wiley & Sons.
- [20]. Muthuselvi, C., M. Dhavachitra and S.Pandiarajan, 2016. Growth and Characterization of Aspirin Crystal in the Phosphoric acid Medium. *Journal of Chemical and Pharmaceutical Research*, 8(5): 804-814.
- [21]. Roseline Sebastian, Sr. S. H., S. Abdul Malek, R. Al-Tamimi, R. Nasser, El-Brollosy, Ali A. El- Emam, C. Yohannan Panicker and Christian Van Alsenoy, (2015). Vibrational spectroscopic (FT-IR and FT-Raman) studies, HOMO–LUMO, NBO analysis and MEP of 6-methyl-1-((2E)-2-methyl-3-phenyl-prop-2-en-1-yl)oxy)methyl)-1,2,3,4-tetrahydro quinazoline-2,4-dione, a potential chemotherapeutic agent, using density functional methods. *Spectrochimica Acta Part A: Molecular and Biomolecular Spectroscopy*, 134: 316-325.
- [22]. Yusuf Sert, S., Sreenivasa, Hatice Dogan, N. R. Mohan, P. A. Suchetan and Fatih Uzun, 2014. Vibrational frequency analysis, FT-IR and Laser-Raman spectra, DFT studies on ethyl (2E)-2-cyano-3-(4-methoxyphenyl)-acrylate, *Spectrochimica Acta Part A: Molecular and Bio Molecular Spectroscopy*, 130: 96-104.
- [23]. Muthuselvi, C., S. Pandiarajan, B. Ravikumar, S. Athimoolam and R. V. Krishnakumar, (2018). Halogen Substituted Indeno Quinoxaline Derivative Crystal: A Spectroscopic Approach. *Asian Journal of Applied Sciences*, 11: 29-37.
- [24]. ChinnaBabu, P., N. Sundaraganesan, S. Sudha, V. Aroulmoji and E. Murano, 2012. Molecular structure and vibrational spectra of Irinotecan: A density functional theoretical study, *Spectrochimica Acta Part A: Molecular and Biomolecular Spectroscopy*, 98: 1-6.
- [25]. Muthuselvi, C., G.Sofiya and S. Pandiarajan, 2017. Structural, Spectral and Antimicrobial Studies on Semi-Organic 4-Carboxyanilinium Perchlorate Monohydrate Crystal. *Journal of Chemical and Pharmaceutical Research*, 9(5):129-137.
- [26]. Anitha, R., S. Athimoolam, M. Gunasekaran and K. Anitha, 2014. X-ray, vibrational spectra and quantum chemical studies on a new semiorganic crystal: 4-Chloroanilinium perchlorate. *Journal of Molecular Structure*, 1076: 115–125.
- [27]. Baran, E.J., I. Viera and M. H. Torre, 2007. Vibrational spectra of the Cu(II) complex of L-asparagine and Lglutamine. *Spectrochim. Acta*, 66A: 114-117.
- [28]. Jahubar Ali, A., S. Thangarasu, S. Athimoolam and S. AsathBahadur, 2013. Factor group, spectroscopic and thermal studies on creatininium hydrogen oxalate monohydrate. *Research Journal of Pharmaceutical, Biological and Chemical Sciences*, 1: 1292-1303.